Prospects to search for E6 isosinglet quarks in ATLAS

7th February 2008

R. Mehdiyev[1,2], S. Sultansoy[2,3], G. Unel[4,5], M. Yilmaz[3]

Abstract

We consider pair production of new down-type isosinglet quarks originating from E_6, which is the favorite gauge symmetry group in superstring inspired GUT models. The study concentrates on the possibility of observing the pair production of the lightest of the new quarks, D, in the ATLAS detector at the forthcoming LHC accelerator, in the channel $D\bar{D} \to ZjZj$. Both signal and background events are studied using tree level event generators based on Monte Carlo techniques. The detector effects are taken into account using the ATLAS fast simulation tool, ATLFAST. It is shown that ATLAS can observe the D quark within the first year of low luminosity LHC operation if its mass is less than 650 GeV. For the case of two years of full luminosity running, 1 TeV can be reached with about three sigma significance.

1 Introduction

If observed, the long awaited discovery of the Higgs particle at the LHC experiments [1, 2] will complete the validation of the basic principles of the Standard Model (SM). However, the well known deficiencies of the SM, such as the arbitrariness of the fermion mass spectrum and mixings, the number of families, the real unification of the fundamental interactions and the origin of baryon asymmetry of the universe require extensions of the SM to achieve more complete theories. In general, these extensions predict the existence of new fundamental particles and interactions. The forthcoming LHC will give the opportunity to explore new colored particles and their interactions to test these predictions. Three types of new quarks (see [3] for a general classification) are of special interest: the fourth SM family quarks, up type and down type weak isosinglet quarks. The existence of the fourth SM family is favored by flavor democracy (see [4] and references therein for details), Q=2/3 quarks are predicted by the little Higgs model [5] and $Q = -1/3$ isosinglet quarks are predicted by Grand Unification Theories (GUTs), with E_6 as the unification group [6]. The GUT models permit solving at least two of the above mentioned problems, namely, the complete unification of the fundamental interactions (except gravity) and the baryon asymmetry of the observed universe by merging strong and electroweak interactions in a single gauge group. Theories adding gravity to the unification of fundamental forces, superstring and supergravity theories [7] also favor E_6 as a gauge symmetry group when compactified from 10 (or 11) dimensions down to the 3+1 that we observe (see [8] and references therein for a review of E_6 GUTs).

For LHC, the production and observation of the first and second type of new quarks have been investigated in [1, 9] and [5, 10] respectively. In this work, we study the possibility to observe the third, down type isosinglet quarks predicted by the E_6-GUT model, at LHC in general, and, specifically in the ATLAS experiment[1] using the 4 lepton and 2 jet channel. The current experimental limit on the mass of an isosinglet quark is $m > 199$ GeV [11]. The detailed study for down type isosinglet quark signatures at the Tevatron has been recently performed in [12] and it has been shown that the upgraded Tevatron would allow a mass reach up to about 300 GeV.

2 The Model

If the group structure of the SM, $SU_C(3) \times SU_W(2) \times U_Y(1)$, originates from the breaking of the E_6 GUT scale down to the electroweak scale, then the quark sector of the SM is extended in the following manner:

---

[1]Université de Montréal, Département de Physique, Montréal, Canada.
[2]Institute of Physics, Academy of Sciences, Baku, Azerbaijan.
[3]Gazi University, Physics Department, Ankara, Turkey.
[4]CERN, Physics Department, Geneva, Switzerland.
[5]University of California at Irvine, Physics Department, USA.

arXiv:hep-ex/0603005v2 18 May 2006

$$\begin{pmatrix} u_L \\ d_L \end{pmatrix}, u_R, d_R, D_L, D_R; \quad \begin{pmatrix} c_L \\ s_L \end{pmatrix}, c_R, s_R, S_L, S_R; \quad \begin{pmatrix} t_L \\ b_L \end{pmatrix}, t_R, b_R, B_L, B_R \quad . \tag{1}$$

As shown, each SM family is extended by the addition of an isosinglet quark. The new quarks are denoted by letters D, S, and B. The mixings between these and SM down type quarks is responsible for the decays of the new quarks.

These mixings increase the number of angles (N_Θ) and phases (N_Φ) with respect to the SM CKM matrix. For a general multi-quark model, one has [13] :

$$\begin{aligned} N_\Theta &= N \times (l + m - \frac{3N+1}{2}) \\ N_\Phi &= (N-1) \times (l + m - \frac{3N+2}{2}) \end{aligned} \tag{2}$$

where l and m are the numbers of the up-type and down-type quarks respectively; and N is the number of $SU(2)_W$ doublets formed by left handed quarks. In the case of the E_6 model, we have $m = 2l = 2N = 6$ and Eq. (2) yields $N_\Theta = 12$ and $N_\Phi = 7$. The special case $m = l + 1 = N + 1 = 4$, considered in [12], yields $N_\Theta = 6$ and $N_\Phi = 3$ which coincides with the number of parameters in the Little Higgs models with one additional isosinglet up-type quark [5] .

In this study, the intrafamily mixings of the new quarks are assumed to be dominant with respect to their inter-family mixings. In addition, as for the SM hierarchy, the D quark is taken to be the lightest one. The usual CKM mixings, represented by superscript θ, are taken to be in the up sector for simplicity of calculation (which does not affect the results). Therefore, the Lagrangian relevant for the decay of the D quark becomes [14] :

$$\begin{aligned} \mathcal{L}_\mathcal{D} &= \frac{\sqrt{4\pi\alpha_{em}}}{2\sqrt{2}\sin\theta_W} \left[\bar{u}^\theta \gamma_\alpha (1-\gamma_5) \, d \cos\phi + \bar{u}^\theta \gamma_\alpha (1-\gamma_5) \, D \sin\phi \right] W^\alpha \\ &\quad - \frac{\sqrt{4\pi\alpha_{em}}}{4\sin\theta_W} \left[\frac{\sin\phi\cos\phi}{\cos\theta_W} \bar{d}\gamma_\alpha (1-\gamma_5) \, D \right] Z^\alpha + h.c. \end{aligned} \tag{3}$$

The measured values of V_{ud},V_{us},V_{ub} constrain the d and D mixing angle ϕ to $|\sin\phi| \leq 0.07$ assuming the squared sum of row elements of the new 3×4 CKM matrix give unity (see[11] and references therein for CKM matrix related measurements). The total decay width and the contribution by neutral and charged currents were already estimated in [14]. As reported in this work, the D quark decays through a W boson with a branching ratio of 67% and through a Z boson with a branching ratio of 33%. The total width of the D quark as a function of its mass is shown in Fig. 1 for the illustrative value of $\sin\phi = 0.05$. It is seen that the D quark has a rather narrow width and becomes even narrower with decreasing value of ϕ since it scales through a $\sin^2\phi$ dependence. If the Higgs boson exists, in addition to these two modes, D quark might also decay via the $D \to H\, d$ channel which is available due to $D - d$ mixing. The branching ratio of this channel for the case of $m_H = 120$ GeV and $\sin\phi = 0.05$ is calculated to be about 25%, reducing the branching ratios of the previously discussed neutral and charged channels to 50% and 25%, respectively [12, 15]. However, this study will not take into account the possible existence of the Higgs boson and will concentrate on the pair production of the D quarks which is approximately independent of the value of $\sin\phi$. One should note that the additional consideration of single production of D quark increases the overall D quark production rate; for example by about 40% for $m_D = 800$ GeV if $\sin\phi = 0.05$. However, final state particles and SM backgrounds are different from the pair production case, making it a rather different process to study.

3   Pair Production at LHC - signal at generator level

The main tree level Feynman diagrams for the pair production of D quarks at LHC are presented in Fig. 2. The $gD\overline{D}$ and $\gamma D\overline{D}$ vertices are the same as their SM down quark counterparts. The modification to the $ZD\overline{D}$ vertex due to $d - D$ mixing can be neglected due to the small value of $\sin\phi$. The Lagrangian in Eq. (3) was implemented into tree level event generators, *Comphep* [16] version 4.3 and *Madgraph* [17] version 2.3 . The total pair production cross sections from these two Monte Carlo generators are shown in Fig. 3. The difference in cross section calculated by these two generators, the first one, based on full matrix element calculation and the other on the numerical methods is less than 5% for the range of D quark mass from 400 to 1400 GeV. The impact of uncertainties in parton distribution functions (PDFs) [18], is calculated by using different PDF sets, to be less than 10% for the same range. For example at $m_D = 800$ GeV and $Q^2 = m_Z^2$, the cross section values are 450 (CompHep, CTEQ6L1) and 468 (CompHep, CTEQ5L) versus 449 (MadGraph, CTEQ6L1) and 459 (MadGraph, CTEQ5L) fb with an error of about one percent. For the same PDF set,

Figure 1: The width of D quark as a function of its mass ($\sin\phi = 0.05$)
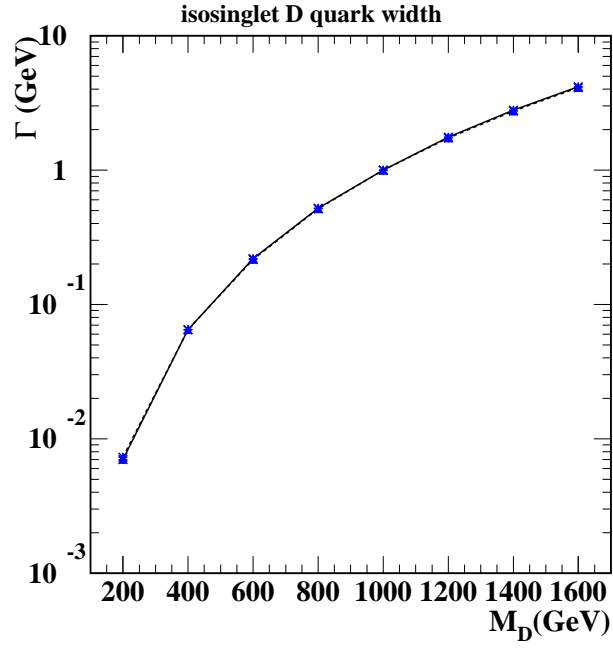
isosinglet D quark width

Figure 2: The tree level Feynman diagrams for the pair production of isosinglet quarks

gluons, s channel

gluons, t channel 1

gluons, t channel 2

up quarks, s channel

down quarks, s channel

up quarks, t channel

down quarks, t channel 1

down quarks, t channel 2

down quarks, t channel 3
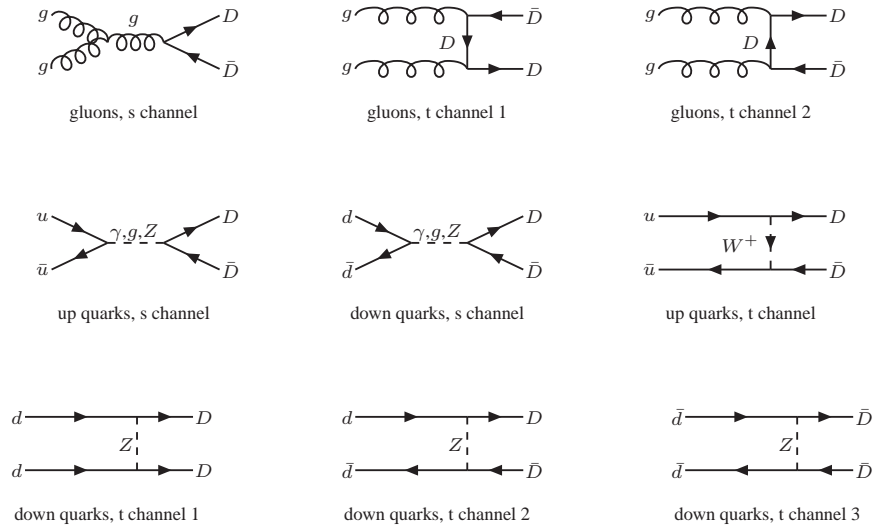
Figure 3: The $D\overline{D}$ pair total production cross section (solid line) as a function of D quark mass is shown as calculated with CompHep (triangles) and with MadGraph (circles). The dashed line is for the gluon contribution and the dotted line is for the quark contribution. The two generators agree within 2% and the effect of PDF uncertainties is computed to be less than 10% through 5 orders of magnitude in the cross section.
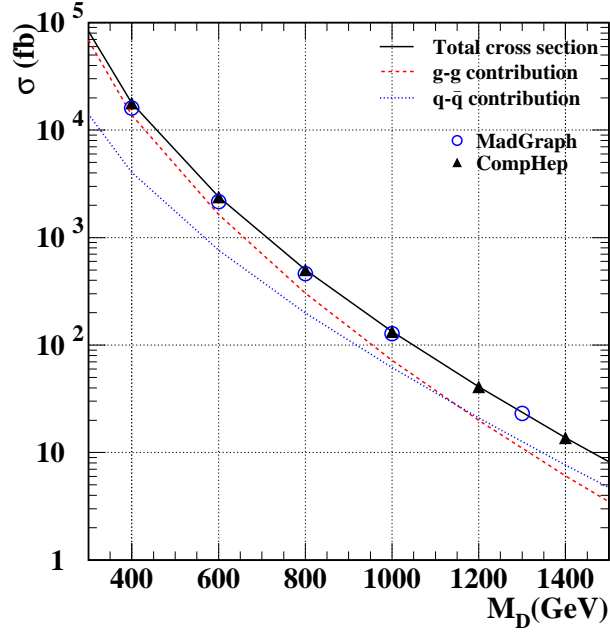
the two programs give the same answer validating both of the MC generators against each other and the implementation of the model. The same figure also contains the partial (gg and $q\bar{q}$) contributions showing that the largest contribution to the total cross section comes from the first three diagrams for D quark masses <1100 GeV, while for higher D quark masses, contributions from s-channel $q\bar{q}$ subprocesses becomes dominant. For these computations, $q\bar{q}$ are assumed to be only from the first quark family since, the contribution to the total cross section from $s\bar{s}$ is about 10 times smaller and the contribution from $c\bar{c}$ and $b\bar{b}$ are about 100 times smaller. The t-channel diagrams mediated by Z and W bosons, shown on the bottom row of Fig. 2, which are suppressed by the small value of $\sin\phi$ (for example 0.4 fb at $m_D = 800$ GeV) are also included in the signal generation.

The isosinglet quarks being too heavy are expected to immediately decay into SM particles. The decay channels leading to possible discovery for the D quark pairs are summarized in Table 1. We have initially focused on the 4 lepton final states of the neutral channel only: although it has the smallest branching ratio, the possibility of reconstructing the invariant mass for Z bosons and thus for both D quarks makes it favorable for a feasibility study. Therefore the final state we would be looking for is composed of two high transverse momenta jets and two Z bosons, all coming from the decay of the D quarks. The high transverse momentum of the jets coming from the D quark decays can be used to distinguish the signal events from the background.

All the SM processes allowed in proton collisions yielding two Z bosons and two jets (originating from any parton except b and t quarks) were considered as background. These can be classified in three categories via the initial state partons: qq, qg and gg where g stands for gluon and q can be any quark or anti-quark from the first two families. The contribution from third quark family is assumed to be negligibly small due to mass and PDF arguments. Although a complete list can be seen in [20], one should note that the 78% of the background cross section originates from the processes in first two categories : $qg \rightarrow qgZZ$ (where $q = u$, d, $\bar{d}$, c, s, $\bar{s}$) contributes 58%, and $q\bar{q} \rightarrow ggZZ$ (where $q = d$, u, s, c) contributes 20%. The simple requirements imposed at the generator level are:

$$
\begin{aligned}
|\eta_p| &< 2.5 , \\
P_{T,p} &> 100 \text{ GeV} , \\
R_{p\bar{p}} &> 0.4 , \\
|\eta_Z| &< 5.0
\end{aligned}
\tag{4}
$$

where R is the cone separation angle between two partons ($p = d, \bar{d}$), η_p and η_Z are pseudorapidities of a parton and Z boson respectively, and $P_{T,p}$ is the parton transverse momentum. The selection of the η region is driven by partonic

4

Table 1: The promising signal channels. The fourth column contains the branching ratios of the SM particles, whereas the last column has the total branching ratios.

$D\bar{D} \rightarrow$	Final State	Expected Signal	Decay B.R.	Total B.R.
$Z\,Z\,d\,\bar{d}$	$Z \rightarrow l\bar{l}\ Z \rightarrow l\bar{l}$	$4\,l\ +2\,jet$	0.07×0.07	0.0005
0.33×0.33	$Z \rightarrow l\bar{l}\ Z \rightarrow vv$	$2\,l\ +2\,jet + \not{E}_T$	$2 \times 0.07 \times 0.2$	0.0028
	$Z \rightarrow l\bar{l}\ Z \rightarrow q\bar{q}$	$2\,l\ +4\,jet$	$2 \times 0.07 \times 0.7$	0.0107
$Z\,W\,d\,u$	$Z \rightarrow l\bar{l}\ W \rightarrow l\bar{v}$	$3\,l\ +2\,jet + \not{E}_T$	0.07×0.21	0.0065
$2 \times 0.33 \times 0.67$	$Z \rightarrow l\bar{l}\ W \rightarrow q\bar{q}$	$2\,l\ +4\,jet$	0.07×0.68	0.0211

spectra pseudorapitidy distributions, which are peaked in the barrel detector area. The signal cross section was calculated with both generators as a function of the D quark mass, but the background only with Madgraph as it is faster in numerical evaluation. For $m_D = 800$ GeV, using the generator level cuts listed in Eq. (4), the cross section of the $ZZ\,2jet$ channel is found to be $\sigma_{signal} = 45.4 \pm 2$ fb (CompHep) whereas the SM background for the same final state particles is $\sigma_{bg} = 345 \pm 17$ fb (MadGraph). Already at this level, a significance of $S/\sqrt{B} \approx 2.4$ can be obtained with an integrated luminosity of 1 fb^{-1}.

4 Observation in ATLAS detector using $4l\,2jet$ channel

Using the preselection cuts listed in the previous section, 5000 signal events at $m_D = 800$ GeV in CompHep and slightly relaxing the jet transverse momentum cut, ($P_{T,j} > 50$ GeV), 40000 background events in MadGraph were generated. The D quarks in signal events were made to decay in CompHep into SM particles. The final state particles for both signal and background events were fed into PYTHIA version 6.218 [21] for initial and final state radiation, as well as, hadronization using the CompHep-Pythia and MadGraph-Pythia interfaces provided by Athena (the ATLAS offline software framework) v9.0.3. To incorporate the detector effects, all event samples were processed through the ATLAS fast simulation tool, ATLFAST [22], and the final analysis has been done using physics objects that it produced.

It must be noted that ATLFAST uses a parameterization for electrons, muons and hadrons without the detailed simulation of showers in the calorimeters. There is also a separate parameterization on the resolution for muons and electron tracks for the inner detector efficiencies. Minimum transverse energy of electromagnetic and hadronic clusters to be considered as electron or jet showers are $E_T > 5$ GeV and $E_T > 10$ GeV, respectively. Electromagnetic and hadronic cells in ATLFAST have the same granularity : $\Delta\eta \times \Delta\phi = 0.1 \times 0.1$. The electron isolation criteria requires a minimum distance $\Delta R \equiv \sqrt{(\Delta\eta)^2 \times (\Delta\phi)^2} \geq 0.4$ from other clusters and a maximum transverse energy deposition, $E_T < 10$ GeV in outer cells accompanying the electron candidate. These outer cells are to be in a cone of radius $\Delta R = 0.2$ along the direction of emission. The jets are reconstructed using the cone algorithm with the $\Delta R = 0.4$ cone size. The smearing of particle clusters and jets is tuned to what is expected for the performance of the ATLAS detector from full simulation and reconstruction using the GEANT package[23].

For this initial feasibility study, where the aim is to reconstruct the invariant mass of both D quarks, only e and μ decays of Z bosons are considered. Although the effective cross section becomes small compared to other decay channels, the benefits of this selection for a clean signal and for correct invariant mass reconstruction are indisputable. Other studies involving the invisible decays of Z boson and leptonic decays of W boson are in preparation. For the initial state particles, gg, $u\bar{u}$ and $d\bar{d}$ sub-channels were studied separately, and for final state particles only light quark jets were considered, all using CTEQ6L1 as PDF [18]. For the case of $M_D = 800$ GeV, the contributions from each sub-channel to the final cross section were about 50 %, 32% and 18% respectively.

4.1 $4l\,2jet$ channel, both $Z \rightarrow \mu\mu$ case

To reconstruct the two Z bosons, four isolated muons were required. The efficiency of finding 4 isolated muons is roughly 50%. Since it is not known which two muons were originating from the same Z boson, all three possible combinations (assuming the lepton charge is not measured) were considered. The reconstructed invariant mass of the muon pairs was required to be close to the Z boson mass: within a window of 20 GeV around the central value of 90 GeV. If all pair combinations happened to be within the mass window, the one with the invariant mass closest to the measured value of Z boson mass was taken. The efficiency of reconstructing two Z bosons was about 90%. High transverse momentum cuts as in equation set below were applied to all leptons and jets to distinguish the signal events from background. One should note that, all the muons in such an event would satisfy the currently set trigger conditions for leptons $P_{T,lepton} \geq 20$ GeV [19]. The momentum distributions for all muons in an event and the imposed cuts for both signal and background can be

Figure 4: The transverse momentum cuts for muons (upper set) and jets (lower set). The plots for signal at $M_D = 800\,\text{GeV}$ and the SM backgrounds are shown with arrows pointing at the cut values. The highest jet P_T for signal events peaks around 300 GeV, whereas for background no such peak is observed.
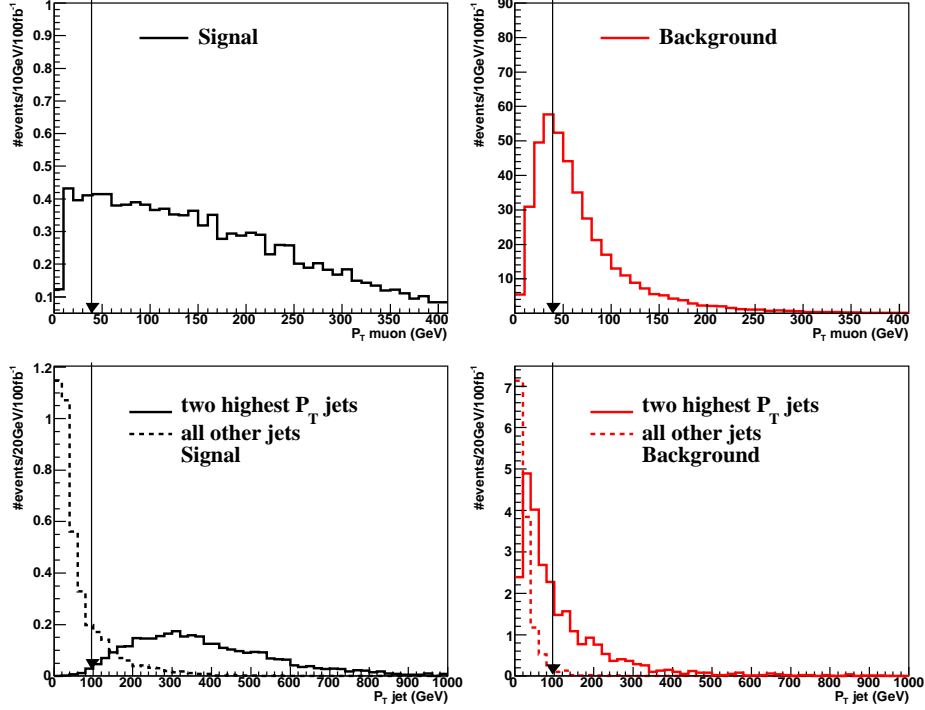

Figure 5: The invariant mass plots for signal at $M_D = 800$ GeV and background events in the $Z \to \mu\mu$ case, obtained from two reconstructed Z bosons and two highest P_T jets.
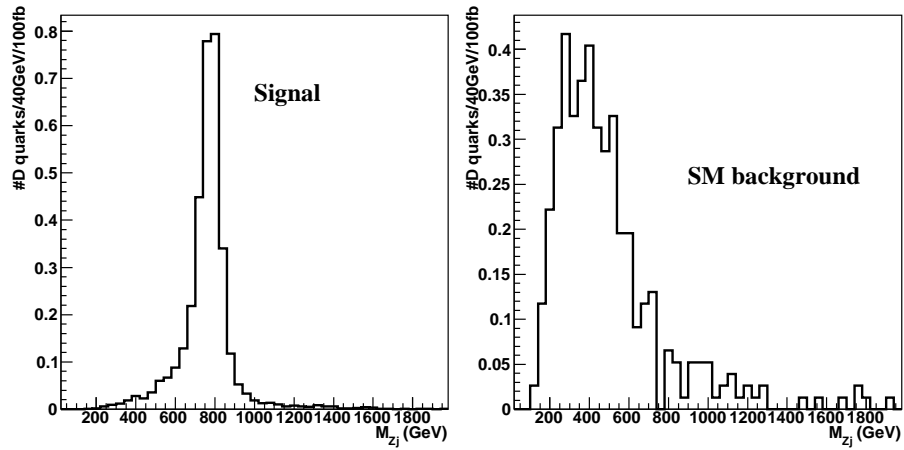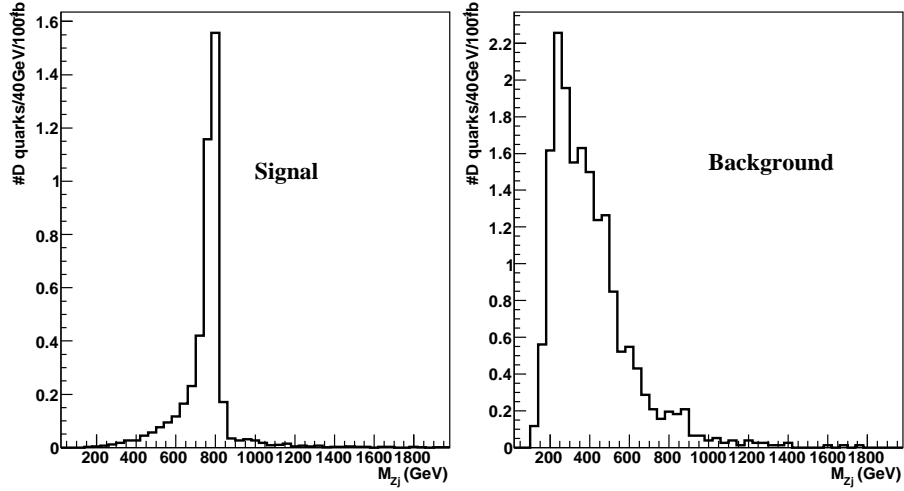
Figure 6: The D quark invariant mass reconstruction in $Z \rightarrow ee$ case for all signal sub-channels as compared to SM background. The signal was generated for $M_D = 800$ GeV.

seen in Fig. 4 upper set where the vertical arrow points at the imposed cut value. The percentage of muons surviving the transverse momentum cut in equation (5) is about 60%. The events with at least two jets with transverse momentum greater than 100 GeV were kept in order to fully reconstruct the invariant mass of D quarks. In the lower set of Fig. 4, the solid line shows the momenta of the two most energetic jets in an event, whereas the dashed curve is for all other jets in the same event, again the vertical arrows pointing at the cut values. The two most energetic jets and the two previously reconstructed Z bosons were combined to reconstruct the D quark pair which was the goal of this study. However, the correct association of the two most energetic jets to the two reconstructed Z bosons is not known and involves combinatorics. Since the mass of the D quark is not known a priori, the "mass window around the central value" method that was used for Z boson reconstruction cannot be applied. The effect of wrong jet-Z association has the impact of enlarging the tails for the signal invariant mass distribution. This problem was partially solved by selecting the combination with the smallest absolute value of the difference between the two reconstructed D quark masses. Reconstructed invariant mass histograms are given separately in Fig. 5 for both signal and background cases. Therefore, the list of all the analysis level cuts becomes:

$$
\begin{aligned}
N_\mu &= 4 \,, \\
P_{T,\mu} &> 40 \text{ GeV} \,, \\
M_Z &= 90 \pm 20 \text{ GeV} \,, \\
N_{jet} &\geq 2 \,, \\
P_{T,jet} &\geq 100 \text{ GeV} \,.
\end{aligned}
\tag{5}
$$

The selection cut efficiencies for both signal and background events are given in Table 2 where each efficiency is calculated relative to the previous one, and the last column contains the combined efficiency value.

Table 2: The individual selection cut efficiencies in percent for the both $Z \rightarrow \mu\mu$ case, for signal and background

channel	N_μ	M_Z	$P_{T,\mu}$	N_{jet}	$P_{T,jet}$	$\epsilon_{combined}$
Signal	48	91	59	100	95	25
Background	34	96	16	96	12	0.6

4.2 $4l\,2jet$ channel, both $Z \rightarrow ee$ case

The cuts for this channel are same as for the channel above (Eq. (5)), except the cut on the transverse momentum of electron, $P_{T,e} > 15$ GeV has been used. The existence of at least one electron originating from the Z boson decay which satisfies the isolated lepton trigger condition has also been checked for all 4 electron events. The method for reconstructing the Z boson and eventually the D quark remains the same as in the previous case. The selection cut efficiencies for this

Figure 7: The D quark invariant mass reconstruction in $ZZ \rightarrow ee\mu\mu$ case for all signal sub-channels as compared to SM background. The signal was generated for $M_D = 800$ GeV.
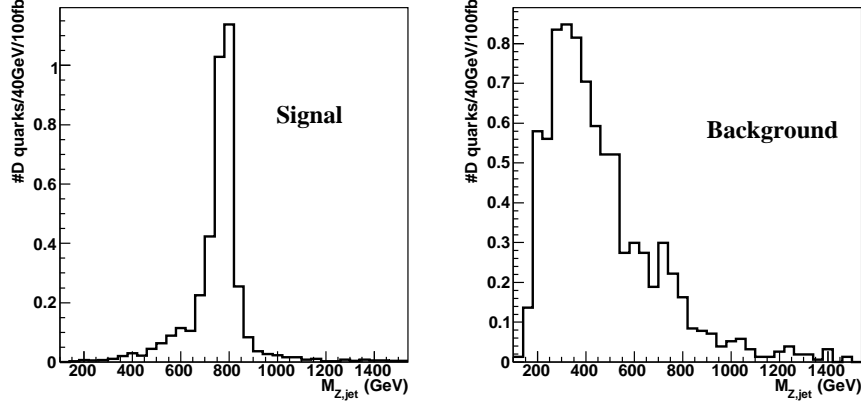
case are shown in Table 3 for both signal and background. The electron cuts leave slightly higher surviving events for both signal and background as compared to the muons. This difference and the different cut values for lepton transverse momenta can be attributed to the over optimistic electron reconstruction in the ATLAS software. The impact of this issue, which was under investigation at the time of this writing, was estimated by comparing the fits to the reconstructed Z bosons from both electrons and muons and was found to be about 5%. The invariant mass spectra is given in Fig. 6 for a bin width of 40 GeV, showing the expected number of signal events being larger than the background ones.

Table 3: The individual selection cut efficiencies in percent for the both $Z \rightarrow ee$ case for both signal and background.

channel	N_e	M_Z	$P_{T,e}$	N_{jet}	$P_{T,jet}$	$\epsilon_{combined}$
Signal	40	99	87	100	95	33
Background	37	98	83	94	7	2.0

4.3 $4l\, 2jet$ **channel, one** $Z \rightarrow ee$ **and one** $Z \rightarrow \mu\mu$ **case**

This case is based on two isolated electrons, two isolated muons and two jets. There is no ambiguity in the lepton selection for Z invariant mass reconstruction thus a simpler reconstruction algorithm suffices. Both muons and at least one electron satisfy the trigger condition. The event selection cuts are summarized in the equation set 6:

$$
\begin{aligned}
N_\mu &= 2 , \quad N_e = 2 , \\
P_{T,\mu} &> 40 \text{ GeV} , \\
P_{T,e} &> 15 \text{ GeV} , \\
N_{jet} &\geq 2 \\
P_{T,jet} &\geq 100 \text{ GeV} , \\
M_Z &= 90 \pm 20 \text{ GeV} ,
\end{aligned}
\tag{6}
$$

The selection cut efficiencies are given in Table 4. Since the branching ratio is higher by a factor of two, compared to the first and second cases, this case yields more signal events and dominates the results. The reconstructed invariant mass for the signal and the SM background is given in Fig. 7 showing that the expected number of signal events is higher than for the background, in the region of the peak.

5 Results

All three above mentioned leptonic reconstruction cases were also considered for systematic studies at other D quark mass values:$M_D = 600, 1000, 1200$ GeV (The details of this analysis can be found in [20]). For values of D quark mass

Table 4: The individual selection cut efficiencies for one $Z \rightarrow ee$ and one $Z \rightarrow \mu\mu$ sub-case. The subscript l represents both electron and muon cases.

channel	N_l	M_Z	$P_{T,l}$	N_{jet}	$P_{T,jet}$	$\epsilon_{combined}$
Signal	44	94	71	100	93	28
Background	35	97	34	95	10	1.1

larger than 900 GeV, in order to increase the expected statistical significance of signal identification, the cuts on the basic kinematic variables were modified as:

$$P_{T,\mu} > 50 \text{ GeV} , \tag{7}$$
$$P_{T,e} > 20 \text{ GeV} ,$$
$$P_{T,jet} > 120 \text{ GeV} .$$

Using the convention of defining a running accelerator year as 1×10^7 seconds, one LHC year at the full design luminosity corresponds to 100 fb^{-1}. For one such year worth of data, all the signal events are summed and compared to all SM background events as shown in Fig. 8. It is evident that for the lowest of the considered masses, the studied channel gives an easy detection possibility, whereas for the highest mass case (M_D=1200 GeV) the signal to background ratio is of the order of unity. If Nature has assigned a high mass to the D quark, other possible detection channels would be either to tag one Z via its leptonic decays and consider the neutrino decays of the other, or would involve hadronic decays of at least one Z and methods to disentangle the jet association. The detailed study of these modes as well as the charged current decay modes is deferred to future work.

For each D quark mass value that was considered, a Gaussian is fitted to the invariant mass distribution around the D signal peak and a polynomial to the background invariant mass distribution. The number of accepted signal (S) and background (B) events are integrated using the fitted functions in a mass window whose width is equal to 2σ around the central value of the fitted Gaussian. The significance is then calculated at each mass value as $S/\sqrt{B}$, using the number of integrated events in the respective mass windows. The expected signal significance for three years of nominal LHC luminosity running is shown in Fig. 9 left hand side. The shaded band in the same plot represents the statistical errors originating from the fact that for each signal mass value, a finite number of Monte Carlo events was generated at the start of the analysis and the surviving events were selected from this event pool. The statistical errors were calculated using binomial distribution and propagated to all significance and luminosity calculations. Given the small value of event yield, the Poisson probability distribution is more appropriate to set the observation and discovery limits [24]. Following the PDG, the Gaussian probabilities for observing 2, 3 and 5 standard deviations when no signal is expected are defined as 4.55%, 0.27% and 5.7$\times 10^{-5}$% respectively. Since the number of observed events in Poisson distribution (and also in experiment) is an integer, the values approaching their Gaussian counterparts from the lower side are taken. Consequently, this procedure always yields more pessimistic luminosity values. For example at $M_D = 800$ GeV, the probability utilized for 3σ limit is 1.34×10^{-3}, about half of its Gaussian counterpart. Therefore, the reach of ATLAS to either exclude the existence of or discover the D quark using the studied dilepton channel is given in Table 5 for different D quark mass values. We observe that for $M_D = 600$ GeV, ATLAS could observe the D quark with a significance more than 3 sigma before the end of the first year low luminosity running (10 fb^{-1}/year) whereas to claim discovery with 5 sigma significance, it would need about 2 years of running time at low luminosity. For $M_D = 1000$ GeV, about two years of high luminosity running is necessary for a 3 sigma signal observation claim. The graphical representation is also given in Fig.9 right hand side.

For these results, a possible source of systematic error is the selection of the QCD scale: although in a complete computation using all possible diagrams including loops this selection becomes irrelevant, this work relies on tree level calculations. An increase in QCD scale from the presently used value of Z boson mass up to D quark mass would mean a decrease in the total cross sections of about 65%. Such a change would also affect the results presented in this work, taking the 3 sigma signal observation limit mass from 1000 GeV down to 840 GeV for two years of high luminosity running. It should also be noted that the detector related backgrounds and the pile-up effects which could be important at high luminosity LHC, are not considered in this work.

6 Conclusions

This study shows that, for a range of D quark mass from 600 to 1000 GeV, ATLAS has a strong potential to find new physics related to E_6 GUT. After three years of design luminosity running, the 5 sigma discovery reach for D quark mass is about 920 GeV . The impact of the assumptions about D quark mass hierarchy and inter-family mixing is minimal: If

Figure 8: Combined results for possible signal observation at $M_D = 600, 800, 1000, 1200$ GeV . The reconstructed D quark mass and the relevant SM background are plotted for a luminosity of 100 fb^{-1} which corresponds to one year of nominal LHC operation. The dark line shows the signal and background added, the dashed line is for signal only and the light line shows the SM background.
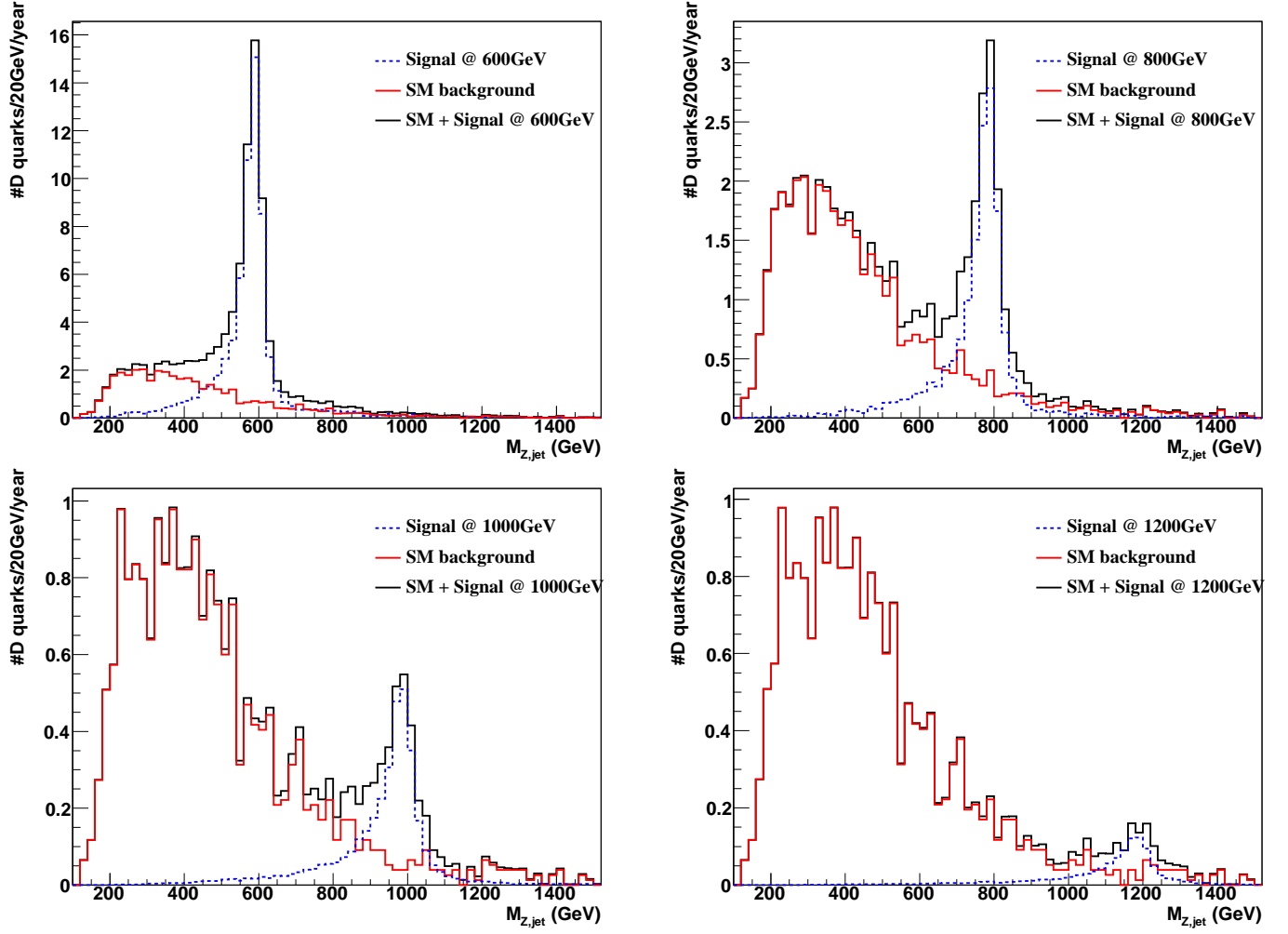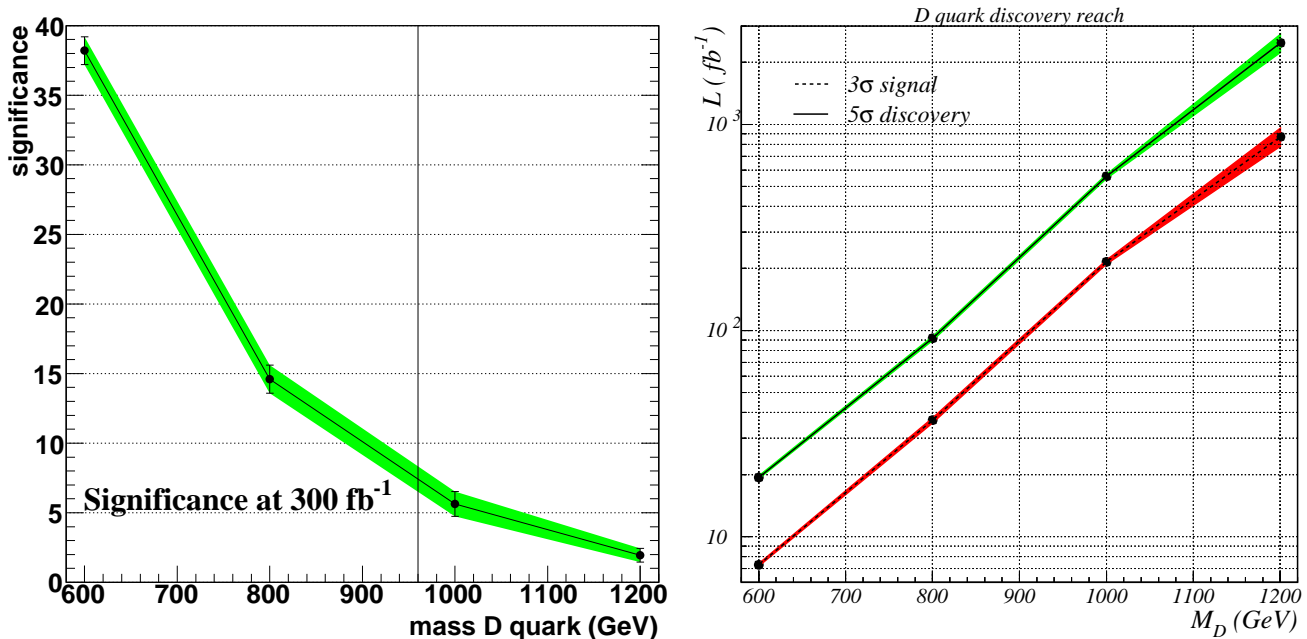

Table 5: The required integrated luminosity in fb^{-1} to discover D quark as a function of its mass is shown. Expected signal and background event number are also given for one year of high luminosity running.

D quark mass (GeV)	600		800		1000		1200	
signal & background events / year	38.2	3.0	9.6	1.3	2.0	0.4	0.6	0.2
Luminosity for 2 σ signal (fb^{-1})	2.4		18.4		86		373	
Luminosity for 3 σ signal (fb^{-1})	7.3		36.7		215		870	
Luminosity for 5 σ signal (fb^{-1})	19.4		91.7		559		2480	

the S quark is the lightest or the D quark mixes mostly to the second family, all the results and conclusions stay as they are. If the third family is involved, either B quark being the lightest or through large mixings to the third quark family, the results would also remain valid, provided no distinction of third family quarks is imposed. However, if the b quarks are to be identified to disentangle the D quark mixing, the $b - jet$ tagging efficiencies should be convoluted with the presented results which would reduce the number of expected signal and background events by at least 50%. To enlarge the experimental reach window for the higher D quark mass values, the inclusion of other channels (remaining lines of the Table 1) is also envisaged. Furthermore, the inclusion of additional gauge bosons predicted by the E_6 group could enhance the signal in the s channel if they have suitable masses. These studies are in preparation.

Figure 9: On the left: the expected statistical significance after 3 years of running at nominal LHC luminosity assuming Gaussian statistics. The vertical line shows the limit at which the event yield drops below 10 events. On the right: the integrated luminosities for 3 sigma observation and 5 sigma discovery cases as a function of D quark mass. The bands represent statistical uncertainties originating from finite MC sample size.

Acknowledgments

References

[1] ATLAS Detector and Physics Performance Technical Design Report. CERN/LHCC/99-14/15.

[2] CMS collaboration, Technical proposal, CERN-LHCC-94-38.

[3] P. H. Frampton, P. Q. Hung and M. Sher, Phys Rep. **330**, *263* (2000).

[4] S. Sultansoy, hep-ph/0004271

[5] N. Arkani-Hamed, A. G. Cohen and H. Georgi. Phys. Lett. B **513**, *232* (2001)., Azuelos, G. et al., Eur. Phys. J. C **39S2**, *13* (2005).

[6] F. Gursey, P. Ramond and P. Sikivie, Phys. Lett. B **60,** *177* (1976); F. Gursey and M. Serdaroglu, Lett. Nuovo Cimento **21**, *28* (1978).

[7] J.H. Schwarz, Lett. Math. Phys. **34** *309* (1995); E. Witten, Nucl. Phys. B **443** *85* (1995) .

[8] J. Hewett and T. Rizzo, Phys. Rep. **183**, *193* (1989).

[9] E. Arik et al., Phys.Rev.D **58**, *117701* (1998).

[10] J.A. Aguilar-Saavedra, Phys.Lett.B **625**, *234* (2005).

[11] S. Eidelmann et. al., P. Phys. Lett. B **592,** *1* (2004).

[12] T. C. Andre and C.L. Rosner, Phys. Rev. D. **69**, *035009*, (2004).

[13] Z. R. Babaev, V.S. Zamiralov and S.F. Sultanov, IHEP preprint, *81-88*, Serpukhov, (1981).

[14] O. Cakir and M. Yilmaz, Europhys. Lett. **38,** *13* (1997).

[15] G. Unel and S. Sultansoy, in preparation.

[16] A. Pukhov, [arXiv:hep-ph/0412191]; E. Boos et al. [CompHEP Collaboration], Nucl. Instrum. Meth. A **534**, *250* (2004).

[17] T. Stelzer and W. F. Long, Phys. Commun. **81**, 357 (1994).

[18] J. Pumplin, D.R. Stump, J. Huston, H.L. Lai, P. Nadolsky and W.K. Tung, JHEP **0207**, 012 (2002) [arXiv:hep-ph/0201195].

[19] ATLAS Collaboration, Trigger and Data Acquisition Technical Design Report, LHCC-2003-022/TDR-016.

[20] R. Mehdiyev et al., ATL-PHYS-PUB-2005-021 (2005).

[21] T. Sjostrand et al., Computer Phys. Commun. **135** (2001) 238 (LU TP 00-30, [hep-ph/0010017])

[22] E. Richter-Was et al., ATLAS Note PHYS-98-131(1998); http://www.hep.ucl.ac.uk/atlas/atlfast/

[23] S. Agostinelli et al., (Geant4 Collaboration), Nucl. Instrum. Meth. A **506,** *250* (2003).

[24] L. Lyons, "Data Analysis for Physical Science Students", Cambridge University Press, 1991.